© 2022. Published by The Company of Biologists Ltd | Journal of Experimental Biology (2022) 225, jeb243272. doi:10.1242/jeb.243272

RESEARCH ARTICLE

The effects of posture on the three-dimensional gait mechanics of human walking in comparison with walking in bipedal chimpanzees

Russell T. Johnson[1,2,*], Matthew C. O'Neill[3] and Brian R. Umberger[4]

ABSTRACT

Humans walk with an upright posture on extended limbs during stance and with a double-peaked vertical ground reaction force. Our closest living relatives, chimpanzees, are facultative bipeds that walk with a crouched posture on flexed, abducted hind limbs and with a single-peaked vertical ground reaction force. Differences in human and bipedal chimpanzee three-dimensional (3D) kinematics have been well quantified, yet it is unclear what the independent effects of using a crouched posture are on 3D gait mechanics for humans, and how they compare with chimpanzees. Understanding the relationships between posture and gait mechanics, with known differences in morphology between species, can help researchers better interpret the effects of trait evolution on bipedal walking. We quantified pelvis and lower limb 3D kinematics and ground reaction forces as humans adopted a series of upright and crouched postures and compared them with data from bipedal chimpanzee walking. Human crouched-posture gait mechanics were more similar to that of bipedal chimpanzee gait than to normal human walking, especially in sagittal plane hip and knee angles. However, there were persistent differences between species, as humans walked with less transverse plane pelvis rotation, less hip abduction, and greater peak anterior–posterior ground reaction force in late stance than chimpanzees. Our results suggest that human crouched-posture walking reproduces only a small subset of the characteristics of 3D kinematics and ground reaction forces of chimpanzee walking, with the remaining differences likely due to the distinct musculoskeletal morphologies of humans and chimpanzees.

KEY WORDS: Bipedalism, Hominin evolution, Morphology, Kinematics, Ground reaction forces, Bent-hip bent-knee

INTRODUCTION

Humans are unique among primates in the habitual use of an upright bipedal walking stride. In general, the gait kinematics and ground reaction forces (GRFs) associated with our body posture during walking include adducted, extended lower limbs with little pelvis rotation, a vertically oriented trunk and a double-peaked (i.e. bi-phasic) vertical GRF (e.g. O'Neill et al., 2015; Rose and Gamble, 2005). The gait mechanics exhibited by humans are distinct from that of common chimpanzees (*Pan troglodytes*; Blumenbach, 1775), who are our closest-living relatives (e.g. Waterson et al., 2005), and are facultative bipeds (e.g. Doran, 1992; Sarringhaus et al., 2014). Bipedal kinematics and GRFs in chimpanzees are characterized by a posture that includes abducted, flexed hind limbs with greater rotations at the pelvis, an anteriorly tilted trunk (e.g. Elftman, 1944; O'Neill et al., 2015) and a single-peaked (i.e. mono-phasic) vertical GRF (Kimura et al., 1977; O'Neill et al., 2022 preprint; Pontzer et al., 2014). There is a longstanding interest in the extent to which the musculoskeletal morphology of the lower back, pelvis and lower/hind limbs underlie these differences in gait mechanics, with implications for the evolution of hominin bipedalism (e.g. DeSilva et al., 2018; Lovejoy et al., 2009; Stern and Susman, 1983). A variety of approaches have been used to try to understand the relationship between morphological structure and gait mechanics, including inferring gait mechanics of fossil hominins based on data from humans walking with crouched postures (Carey and Crompton, 2005; Crompton et al., 1998; Foster et al., 2013; Li et al., 1996; Raichlen et al., 2010; Wang et al., 2003; Yamazaki et al., 1979).

For this study, 'posture' is defined as the general orientation of the body during walking (e.g. upright or crouched), while the term 'gait mechanics' refers to specific variables (e.g. joint angles or GRFs) that change throughout the stride. Previous studies of human crouched posture have sought to emulate bipedal chimpanzee walking (Li et al., 1996; Yamazaki et al., 1979) and/or to test hypotheses about fossil hominin walking (Carey and Crompton, 2005; Crompton et al., 1998; Foster et al., 2013; Raichlen et al., 2010). These studies have focused solely on manipulating and measuring sagittal plane kinematics and kinetics. Yet, adopting broad changes in posture in the sagittal plane may affect gait mechanics in non-sagittal planes. Humans can be provided with instructions to walk with a crouched posture that imitates sagittal plane chimpanzee hind limb kinematics (Foster et al., 2013), but it is unknown whether the non-sagittal plane gait kinematics or GRFs for crouched walking in humans are similar to that of bipedal chimpanzees. The differences in musculoskeletal structure between humans and chimpanzees could lead to differences in the overall three-dimensional (3D) gait mechanics of crouched human walking and chimpanzee bipedal walking, which would imply a key limitation of manipulating posture in humans to infer how extinct hominins, with distinct musculoskeletal morphologies, would have walked.

In addition to a lack of quantitative data on the 3D nature of crouched-posture walking in humans, no studies focused on the evolution of bipedalism have altered trunk orientation during crouched limb walking. However, trunk flexion represents a salient difference between human and bipedal chimpanzee gait (O'Neill et al., 2015; Pontzer et al., 2014; Thompson, 2016). The anterior–trunk flexion in a bipedal chimpanzee shifts the whole-body center of mass forward, which may contribute to their flexed-limb posture (Lovejoy, 2005; Lovejoy and McCollum, 2010; Napier, 1967). Anterior trunk flexion in humans has been shown to affect lower

[1]Department of Kinesiology, University of Massachusetts Amherst, Amherst, MA 01003, USA. [2]Division of Biokinesiology and Physical Therapy, University of Southern California, Los Angeles, CA 90033, USA. [3]Department of Anatomy, Midwestern University, Glendale, AZ 85308, USA. [4]School of Kinesiology, University of Michigan, Ann Arbor, MI 48109, USA.

*Author for correspondence (rtjohnso@usc.edu)

R.T.J., 0000-0002-3026-6307; B.R.U., 0000-0002-5780-2405; M.C.O., 0000-0001-9614-7813

Received 30 July 2021; Accepted 24 January 2022

limb kinematics and vertical GRF patterns (Aminiaghdam et al., 2017; Grasso et al., 2000; Kluger et al., 2014; Saha et al., 2008), although the most substantial effects require more extreme anterior trunk flexion (i.e. 50–90 deg relative to vertical) than observed in either bipedal chimpanzees (i.e. approximately 30–35 deg; Pontzer et al., 2014) or in other primates walking bipedally, such as macaques (i.e. approximately 25 deg; Ogihara et al., 2010). As such, it remains unclear how effects of moderate anterior trunk flexion characteristic of bipedal walking in non-human primates affect gait mechanics in humans. Further, the combined effects of trunk flexion and flexed limb posture on 3D human gait kinematics and GRFs is unknown.

Along with the documented flexed-limb posture during chimpanzee bipedal walking, there is also substantial non-sagittal plane motion that distinguishes it from normal human walking. Chimpanzees exhibit greater range of motion (ROM) than humans for some non-sagittal plane kinematic variables when walking at matched dimensionless speeds (O'Neill et al., 2015), yet perhaps the most striking difference is that pelvis list for chimpanzees is completely out of phase with the pelvis list pattern in human walking. In the single-support period, bipedal chimpanzees elevate their pelvis on the swing limb side, whereas humans drop their pelvis on the swing limb side (Jenkins, 1972; O'Neill et al., 2015). Despite the opposite phasing of pelvis motion, this feature has not been included in human crouched-posture studies. As such, it is unclear whether having humans emulate chimpanzee frontal plane pelvis motion during crouched-posture walking will result in 3D hip joint kinematics or GRF patterns like those observed in chimpanzees. However, even with multiple instructions given to humans to emulate chimpanzee gait mechanics, it is likely that some differences will persist given morphological differences between species.

Human lower limb, pelvis and trunk posture can be easily manipulated during short bouts of gait by providing instructions and feedback to participants, while the underlying musculoskeletal system remains the same (e.g. Carey and Crompton, 2005; Foster et al., 2013; Grasso et al., 2000; Kikel et al., 2020). As such, human crouched-posture gait studies have the potential to provide important insights into how distinct morphological features between species contribute to differences in gait mechanics. However, a full 3D accounting of differences in gait kinematics and GRFs across postures is required, as crouched bipedal walking may have substantial motion and forces outside of the sagittal plane, as exhibited by chimpanzees (O'Neill et al., 2015; O'Neill et al., 2022 preprint). Quantifying these differences will lead to a greater understanding of the effect of posture on gait mechanics and allow for inferences about how the morphology of humans and chimpanzees gives rise to their distinct gait patterns.

Here, we instructed humans to walk with a series of crouched postures to evaluate how instructions focused on lower limb flexion, anterior trunk flexion and pelvis motion lead to alterations in the 3D pelvis and lower limb kinematics and GRFs. Specifically, we collected 3D gait data for (i) normal human walking, (ii) walking with a crouched limb (CL), (iii) walking with a crouched limb and anteriorly flexed trunk (CLT), and (iv) walking with a crouched-limb, anteriorly flexed trunk and a chimpanzee-like pelvis list pattern (CLTP). We chose to manipulate pelvis list, rather than another frontal or transverse plane angle, because the pattern of pelvis list is strikingly out of phase between normal human and chimpanzee gait. The normal and three crouched-posture conditions for humans were compared with previously collected bipedal chimpanzee data to determine the degree to which crouched-posture human walking is similar to that of chimpanzees (O'Neill et al., 2015; O'Neill et al., 2022 preprint). We predicted that the normal human walking condition would be the least similar to chimpanzee gait mechanics out of all human conditions. We further predicted that the CL, CLT and CLTP conditions would lead to progressively more chimpanzee-like gait mechanics through changes in hip flexion and knee flexion motion during the CL and CLT conditions, and additional changes in pelvis list and hip abduction motion for the CLTP condition.

MATERIALS AND METHODS

Human protocol

Ten healthy human subjects (5 female, 5 male; age: 27±5 years; height: 1.70±0.08 m; mass: 68±11 kg; lower limb length: 0.88 ±0.04 m) were recruited for this study. All subjects had no history of gait pathologies, cardiovascular disease, neurological disease or orthopedic problems that would affect how they walked. We recruited recreationally active subjects, who self-reported that they performed at least 150 min of physical activity per week (Garber et al., 2011), to reduce the risk of fatigue being a factor during our data collection. Prior to participating, subjects read and signed an informed consent document approved by the University of Massachusetts Amherst Institutional Review Board. Subjects also completed a Physical Activity Readiness Questionnaire to assess their readiness to participate in the study (Thomas et al., 1992; Warburton et al., 2011).

For each subject, height, mass, age and lower limb length were recorded. Retro-reflective markers were attached to anatomical landmarks on the upper body, pelvis and lower limbs, and clusters of non-colinear markers were placed on the thigh, shank and heel of each lower limb (Fig. 1B) (O'Neill et al., 2015). Subjects were instructed to walk at a comfortable pace for 200 m (five back-and-forth laps, each 20 m length) in the lab to assess their preferred gait speed. Gait speed was measured using two photoelectric sensors placed 6 m apart in the middle of the walkway. The 6 m speed was recorded during the last four laps of the 200 m walk and averaged across the four trials to calculate the preferred gait speed. The measurement of preferred speed and all subsequent experimental trials were performed barefoot by each subject, to match the chimpanzee conditions.

Data were collected from the human subjects walking under four different postural conditions to facilitate comparisons with existing chimpanzee gait (O'Neill et al., 2015; O'Neill et al., 2022 preprint). The four human postural conditions were designated: (1) normal, (2) crouched-limb (CL), (3) crouched-limb, flexed-trunk (CLT) and finally (4) crouched-limb, flexed-trunk, pelvis list (CLTP). The CLTP condition involved providing instructions specific to replicating the frontal plane pelvis motion observed in chimpanzees, which is an out-of-phase pattern compared with typical normal human gait (O'Neill et al., 2015). Each condition was performed at two speeds: the preferred gait speed and at a speed that matched the average, absolute dimensional walking speed for the previously collected chimpanzee data (chimpanzee speed: 1.09 m s^{-1}). The order of the postural conditions was performed in sequence because of the additive nature of the instructions; however, the order of the two speeds was balanced among subjects within each condition (five did the chimpanzee-matched speed first for each condition).

Before beginning the walking trials, a static calibration trial was collected for the purpose of scaling a generic human musculoskeletal model to the size of each subject. For the normal condition, subjects were instructed to 'walk normally' at the given speeds. Next, the CL condition was meant to replicate, as best as

Journal of Experimental Biology (2022) 225, jeb243272. doi:10.1242/jeb.243272

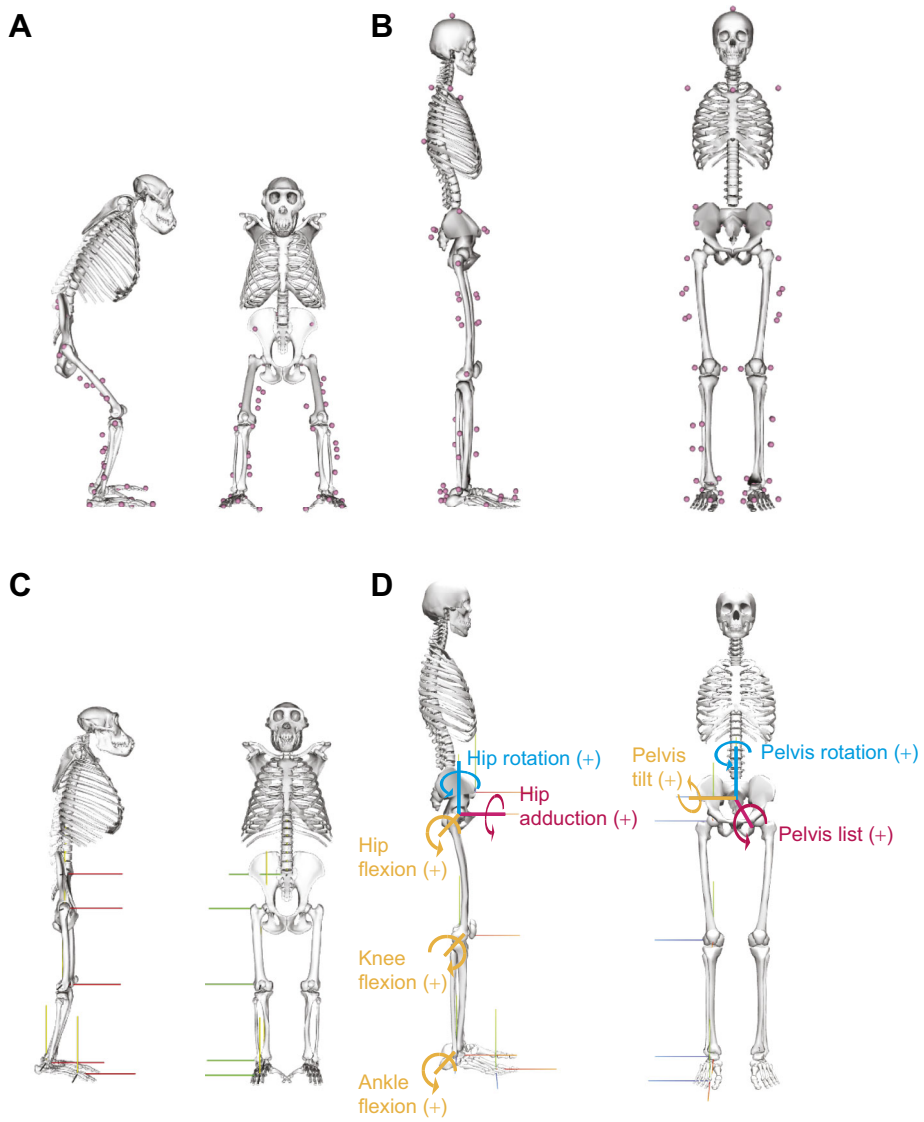

Fig. 1. Musculoskeletal morphology and marker placement. (A,B) Representations of the skeletal morphology and marker positions for the chimpanzee model (A), along with the skeletal morphology and marker positions for the human model (B). The anatomical markers and segment marker clusters are depicted with pink dots. (C,D) The local coordinate systems of the pelvis and lower limbs for the chimpanzee model (C) and human model (D). Each model is positioned with neutral coordinates, where yellow axes represent the *x*-direction, red axes represent the *y*-direction and green axes represent the *z*-direction. The direction of the arrow indicates the positive value for that degree of freedom. The degrees of freedom (DOF) for the human model are labeled in D, and match the chimpanzee model.

possible, the designs from previous two-dimensional crouched-posture studies that focused on sagittal plane variables (Carey and Crompton, 2005; Foster et al., 2013). Prior to the CL condition, the shoulder height of the subject was measured while standing crouched with the hip flexed 50 deg and the knee flexed 30 deg using a large goniometer. A taut rope was stretched along the walkway at this measured shoulder height. Subjects were instructed to 'walk while bending at the hips and knees to match the target rope height' at the given speed. Next, the CLT condition was designed to target the difference in trunk angle between humans and chimpanzees during bipedal gait, and was based on the average bipedal chimpanzee trunk angle (Pontzer et al., 2014). The height of the rope was reset based on the shoulder height of the subjects while standing with the trunk flexed forward 30 deg from the vertical, the hip flexed 50 deg and the knee flexed 30 deg. Subjects were instructed to 'walk while bending at the trunk, hips and knees to match the target rope height' at the given speed. For the final condition (CLTP), the height of the rope remained the same as in CLT and each subject was instructed to 'walk like you did in the previous condition, but now focus on pitching your trunk and pelvis over the supporting limb during the swing phase'. Subjects also viewed a short, animated video of a chimpanzee walking bipedally to help them understand the desired pelvis list pattern. This condition was specifically designed to address the out-of-phase pelvis list motion in chimpanzees relative to normal human gait (O'Neill et al., 2015).

Each of the eight conditions (four postures times two speeds) was performed by the subjects as they walked overground across a walkway with three embedded force platforms (AMTI, Watertown, MA, USA) while GRFs were recorded at 1200 Hz. Kinematic data were collected simultaneously at 240 Hz using an 11-camera motion capture system (Qualisys, Gothenburg, Sweden). Both the 3D raw marker trajectories and GRF data were smoothed using a fourth order zero-lag low-pass Butterworth filter with a cut-off frequency of 6 Hz.

Before each of the conditions, subjects were instructed to practice each walking task for at least three bouts and had the opportunity to ask questions about the instructions. The practice bouts were deemed to be completed once subjects were readily able to reproduce the specified posture and speed. Following the practice bouts, three acceptable trials were recorded for each of the eight conditions. A trial was considered acceptable if: (i) the gait speed was within 3% of the target speed, (ii) the feet cleanly struck each of the three force plates in the correct sequence, and (iii) the subject

maintained the target posture throughout the trial. Maintenance of the target posture was assessed visually, with the help of the rope stretched along the walkway. Subjects were given the opportunity to rest between trials to minimize the chance of becoming fatigued during the data collection. Subjects self-reported that they did not become fatigued by the end of the data collection.

A 3D model of the human musculoskeletal system (Lai et al., 2017) was used to determine the kinematic patterns using OpenSim software (Delp et al., 2007; Seth et al., 2018). The human model had 21 mechanical degrees of freedom (DOF), with a 6 DOF pelvis segment that articulates with a rigid segment representing the head, arms and trunk via a ball-and-socket joint (Fig. 1D). Pelvis angles were calculated in the global reference frame relative to a neutral position for the human and chimpanzee gait data, and were calculated with a rotation–list–tilt sequence (Baker, 2001). As defined by Baker (2001): pelvis rotation is described by 'the angle of rotation of the pelvis about a vertical axis' and pelvis tilt is 'the angle of rotation about the medio-lateral axis of the pelvis'. Pelvis obliquity is 'the angle of rotation of the medio-lateral axis of the pelvis out of the horizontal plane'; in this study, we use the term 'list' rather than 'obliquity' to match with terminology common to OpenSim models. Each lower limb articulated to the pelvis via a ball-and-socket hip joint, the knee was represented as a modified hinge joint that included the translation of the tibia relative to the femur (Yamaguchi and Zajac, 1989), while the ankle and metatarsophalangeal joints were modeled as hinge joints. Lastly, to compare human trunk kinematics between postural conditions and confirm that the subjects were performing the tasks as instructed, trunk segment angles were calculated relative to the horizontal global reference frame.

For each of the 10 subjects, a generic model was scaled to best match the individual anthropometrics of the subject based on the static, standing calibration trial. The scaled model was then used to calculate the generalized coordinates for each trial using the inverse kinematics algorithm in OpenSim (Lu and O'Connor, 1999). The pelvis rotation, pelvis list, pelvis tilt, hip flexion, hip adduction, hip rotation, knee flexion and ankle flexion angles from the inverse kinematics analysis, and the vertical, anterior–posterior and medial–lateral GRFs were compared with corresponding chimpanzee bipedal gait data. For the crouched-posture conditions, subjects were instructed to modify their pelvis list, hip flexion and knee flexion angles; thus, these variables were expected to change directly with the instructions. However, we expected that these instructions would also lead to changes in other kinematic variables, as well as the GRFs.

Chimpanzee protocol

The chimpanzee kinematic and GRF data were drawn from previously published studies (O'Neill et al., 2015; O'Neill et al., 2022 preprint). Therein, three male common chimpanzees (*Pan troglodytes*; age: 5.5±0.2 years; mass: 26.5±6.7 kg; hind limb length: 0.39±0.02 m) walked overground while 3D kinematic data were recorded at 150 Hz and GRF data were recorded at 1500 Hz. The 3D marker trajectories were filtered using a fourth order zero-lag low-pass Butterworth filter, with cut-off frequencies set within the range 4–6 Hz based on visual inspection of the data and the GRFs were low-pass filtered at 60 Hz. Each chimpanzee was trained to walk bipedally using a food reward and positive reinforcement for at least 6 months before data collection began. Four trials were collected per chimpanzee, while they walked at a self-selected speed following an animal trainer offering a food reward. Following data collection, a generic chimpanzee musculoskeletal model (O'Neill et al., 2013) was scaled to each individual chimpanzee using a short series of video frames obtained during the double support period. The chimpanzee musculoskeletal model had 16 mechanical DOF representing the hind limbs and pelvis segment (Fig. 1A). The mechanical DOF in the chimpanzee model were consistent with the human musculoskeletal model for the pelvis, hips, knees and ankles (Fig. 1C). For comparison with the human data, the corresponding chimpanzee angles and GRFs were used for the statistical analyses.

Output variables and statistical analyses

For each of the trials for each of the subjects, the following variables were calculated. Stride length was calculated as the anterior–posterior pelvis displacement during the stride, stride time was the total time that it took to complete the stride, and gait speed was the stride length divided by stride time. Step width for each trial was calculated as the medial–lateral distance between the average centers of pressure under each foot during stance phase (Donelan et al., 2001). The minimum and maximum joint angles were calculated from the averaged time-normalized subject data for each condition, and the ROM was calculated as the difference between the minimum and maximum joint angle.

The eight kinematic variables and three GRF variables described above for each of the four different human posture conditions were compared with the chimpanzee bipedal gait mechanics (for both speeds: normal versus chimpanzee, CL versus chimpanzee, CLT versus chimpanzee, and CLTP versus chimpanzee). The kinematic data for each trial were time normalized to the full stride, and GRF data for each trial were time normalized to the stance phase. The time-normalized data were averaged across trials for each condition for each subject, then group averages were calculated for each condition. The timing of GRF data was normalized to the stance phase, rather than the full stride, so that the comparisons would not be affected by the swing phase when all forces are zero. The magnitude of the GRF data was normalized to body weight. Similarities in pattern and differences in magnitude for the kinematic and GRF variables were evaluated using zero-lag cross-correlations (r) and root-mean-square deviations (RMSD) based on the group average data:

$$r = \frac{\sum_{t=1}^{N}(x_t \cdot y_t)}{\sqrt{\sum_{t=1}^{N}|x_t|^2 \cdot \sum_{t=1}^{N}|y_t|^2}}, \quad (1)$$

and

$$\mathrm{RMSD} = \sqrt{\frac{\sum_{t=1}^{N}(x_t - y_t)}{N}}, \quad (2)$$

where the segment, joint or GRF value at time t is given as x_t (humans) and y_t (chimpanzees) with N data points (N=101). Values for r could vary from −1 to 1, and a greater positive value of r (closer to 1) would indicate that two variables were more similar to each other in pattern throughout the gait cycle. The minimum value for RMSD is 0, which would indicate that the variables have identical values throughout the gait cycle, while greater RMSD values indicate greater differences in magnitude between the two species. Four unique outcome measures were computed for each condition to assess the similarity between human and chimpanzee gait mechanics: (i) the average of r across the eight kinematic variables, (ii) the average of RMSD across the eight kinematic variables, (iii) the average of r for the three orthogonal components of the GRFs, and (iv) the average of RMSD for the three orthogonal components of the GRFs.

Journal of Experimental Biology (2022) 225, jeb243272. doi:10.1242/jeb.243272

Table 1. Spatiotemporal results for the four human conditions (chimpanzee-matched speed) and the chimpanzee bipedal gait

Condition	Velocity (m s^{-1})	Stance time (s)	Swing time (s)	Stride length (m)	Stride frequency (Hz)	Step width (m)	Duty factor
Chimpanzee	1.09±0.10	0.45±0.09	0.27±0.03	0.78±0.07	1.43±0.23	0.26±0.04	0.62±0.03
Normal	1.11±0.03	0.73±0.04	0.40±0.02	1.24±0.06	0.89±0.04	0.14±0.03	0.65±0.01
CL	1.10±0.02	0.75±0.04	0.37±0.03	1.23±0.05	0.91±0.06	0.17±0.04	0.67±0.01
CLT	1.10±0.02	0.75±0.04	0.37±0.03	1.23±0.06	0.90±0.05	0.17±0.05	0.67±0.01
CLTP	1.10±0.02	0.77±0.05	0.39±0.04	1.27±0.09	0.88±0.06	0.21±0.07	0.66±0.02

CL, crouched-limb; CLT, crouched-limb, flexed-trunk; CLTP, crouched-limb, flexed-trunk, pelvis list. Data are means±s.d.

RESULTS

The average preferred gait speed for the 10 human subjects was 1.30 ±0.15 m s^{-1}. During the chimpanzee dimensional speed-matched trials, the human subjects were able to closely match (normal condition speed: 1.11±0.03 m s^{-1}) the average chimpanzee bipedal speed (O'Neill et al., 2015; 1.09±0.10 m s^{-1}; Table 1). There were only subtle differences in kinematics and GRFs between the two human speeds for each posture condition; therefore, only the results comparing the chimpanzee gait data with human gait at the chimpanzee-matched speed are reported in the following sections (see Figs S1–S3 and Tables S1–S3 for corresponding results for human preferred speed to chimpanzee gait). In the spatiotemporal domain, the chimpanzees took shorter and quicker strides than the humans across all posture conditions (Table 1; Table S1). The stance time, stride length and stride frequency were similar across the human posture conditions. Chimpanzees walked with a greater step width (0.26±0.04 m) than any of the human conditions; however, humans had wider steps in the crouched-posture conditions than in the normal condition (range: 0.14±0.03 m for normal to 0.21 ±0.07 m for CLTP), both in absolute terms and relative to hind limb length. A visual summary of each of the human posture conditions and the bipedal chimpanzees is shown in Fig. 2.

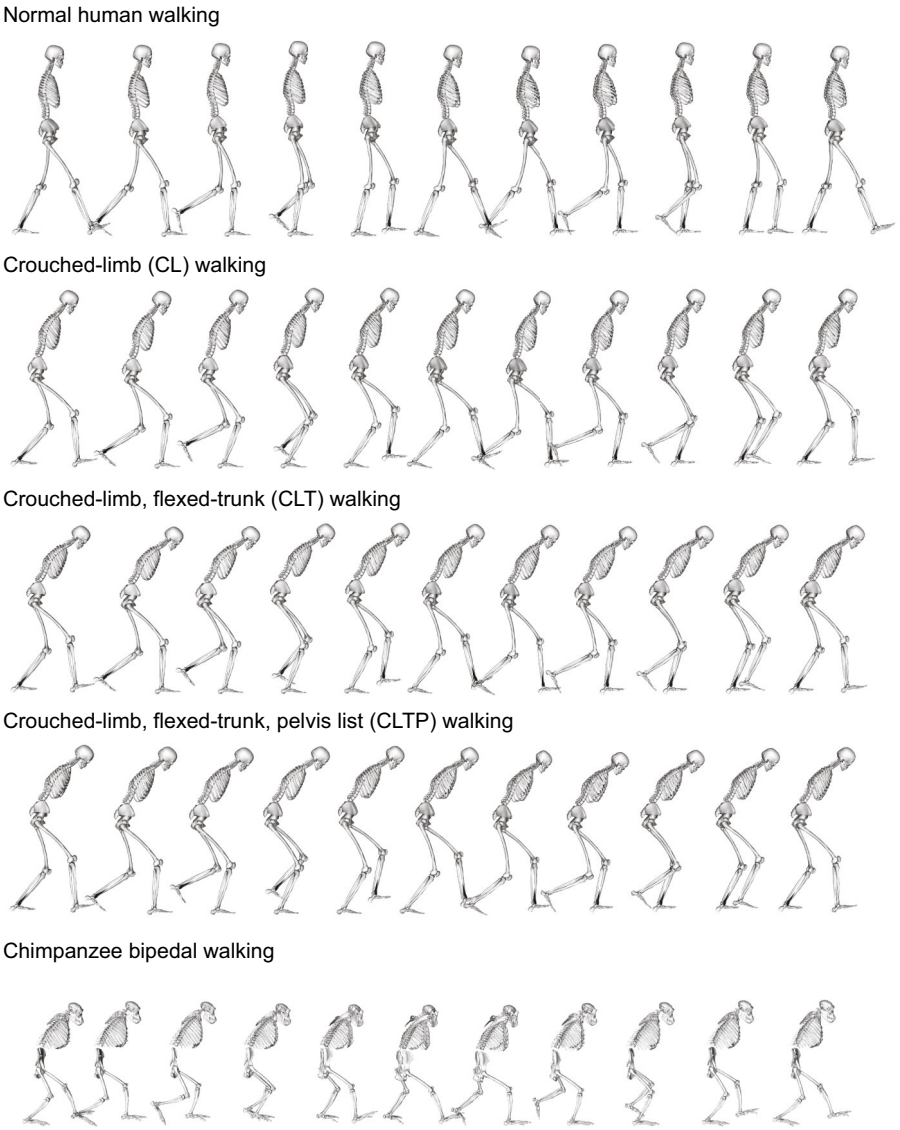

Fig. 2. Time-lapse images. Data from a representative subject were used to create the time-lapse images for each of the four human conditions. A representative chimpanzee trial is presented at the bottom for comparison.

Journal of Experimental Biology (2022) 225, jeb243272. doi:10.1242/jeb.243272

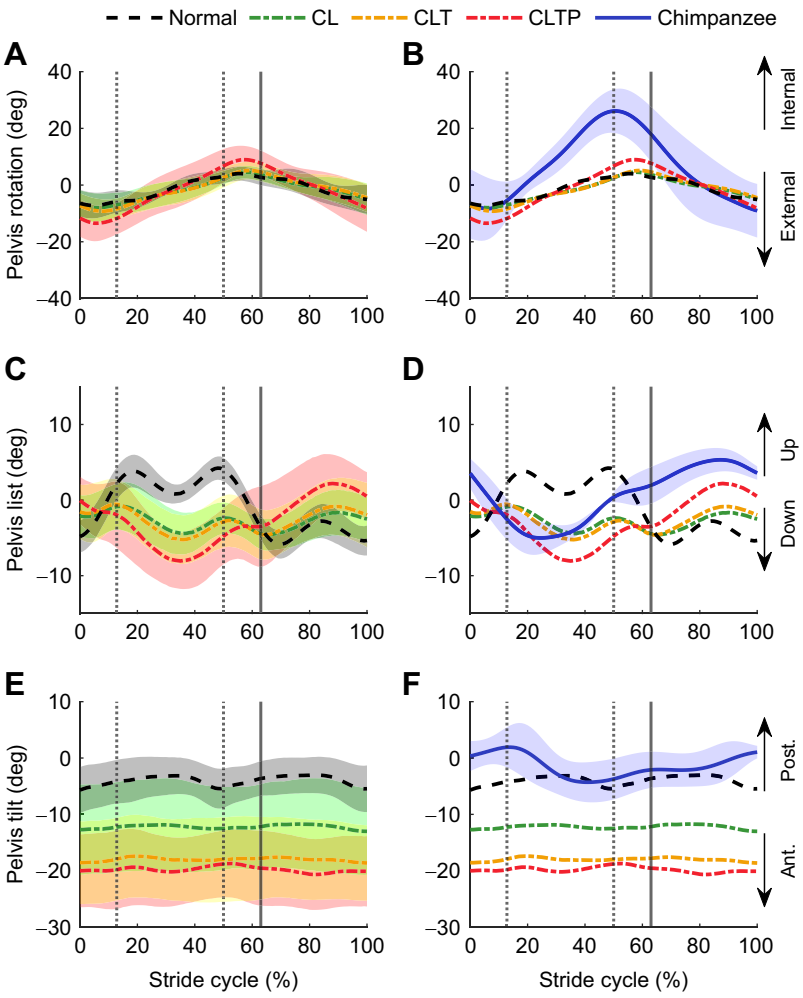

Fig. 3. Pelvis kinematics. Left: mean pelvis rotation (A), list (C) and tilt (E) kinematics for each of the four human conditions (chimpanzee-matched speed; normal, CL, CLT, CLTP); the shaded regions represent 1 s.d. of the mean. Right: mean pelvis rotation (B), list (D) and tilt (F) for each of the four human conditions along with the mean and s.d. for the chimpanzee data. The vertical lines depict left toe-off, left foot strike and right toe-off respectively. Ant., anterior; Post. posterior. Table S1 provides exact gait events across conditions.

Pelvis kinematics

Both the human and chimpanzee subjects internally rotated their pelvis during the first half of the gait cycle, followed by external pelvis rotation during the second half of the gait cycle (Fig. 3A,B). However, the chimpanzees had greater pelvis rotation ROM (46 ±12 deg) over the gait cycle than for any of the human conditions (Table 2). The pelvis rotation ROM was greatest in the CLTP condition than in the other human conditions (24±9 deg). The CLTP human posture condition produced the most chimpanzee-like pelvis rotation motion in pattern (r=0.61) and magnitude (RMSD=10.8 deg) compared with the other human posture conditions (Table 3).

In the frontal plane during normal gait, the human pelvis listed downward towards the swing side limb, whereas the chimpanzees

Table 2. Segment and joint angle minimum, maximum and range of motion (ROM) for each of the conditions

Condition		Pelvis rotation (deg)	Pelvis list (deg)	Pelvis tilt (deg)	Hip flexion (deg)	Hip adduction (deg)	Hip rotation (deg)	Knee flexion (deg)	Ankle flexion (deg)
Normal	Min.	−5±3	−5±2	−7±4	−10±6	−11±3	−13±4	5±2	−14±5
	Max.	8±4	7±2	−2±3	31±4	8±2	−2±4	64±4	16±4
	ROM	12±5	12±3	4±1	42±2	19±4	11±3	59±2	30±4
CL	Min.	−5±2	0±3	−14±8	18±18	−10±5	−9±3	32±6	0±5
	Max.	9±4	6±2	−11±8	58±12	−1±4	2±3	86±7	34±5
	ROM	14±4	6±2	3±1	40±8	9±4	11±3	55±7	35±5
CLT	Min.	−6±3	0±3	−20±7	30±11	−10±5	−10±4	32±2	−2±5
	Max.	10±4	6±4	−16±7	66±7	−1±5	4±4	90±7	35±6
	ROM	15±6	6±3	3±1	36±5	9±3	13±4	59±6	37±6
CLTP	Min.	−10±5	−3±3	−22±6	29±10	−15±6	−13±5	34±5	−3±7
	Max.	14±6	9±5	−18±6	68±8	−5±5	2±5	90±8	35±8
	ROM	23±9	12±4	4±2	40±7	9±3	16±4	56±8	39±9
Chimpanzee	Min.	−12±7	−6±1	−5±4	25±9	−30±3	−35±3	14±3	−19±8
	Max.	29±12	6±1	3±3	52±6	−14±7	4±4	92±2	19±4
	ROM	41±13	12±2	8±1	27±4	16±4	39±2	78±1	38±5

Min., minimum; Max., maximum; ROM, range of motion. Data are means±s.d.

Journal of Experimental Biology (2022) 225, jeb243272. doi:10.1242/jeb.243272

Table 3. Cross-correlation coefficients (*r*) and root-mean-square deviation (RMSD) for kinematics for humans walking (chimpanzee-matched speed) compared with chimpanzee gait

	Human condition vs chimpanzee	Pelvis rotation	Pelvis list	Pelvis tilt	Hip flexion	Hip adduction	Hip rotation	Knee flexion	Ankle flexion	Average
r	Normal	0.56	−0.80	0.53	0.73	0.17	0.83	0.92	0.61	0.44
	CL	0.43	−0.11	0.57	0.98	0.88	0.91	0.99*	0.73	0.67
	CLT	0.43	0.05	0.58*	0.99*	0.94	0.85	0.99*	0.72	0.69
	CLTP	0.61*	0.54*	0.57	0.99*	0.99*	0.95*	0.99*	0.76*	0.80*
RMSD (deg)	Normal	11.8	6.8	3.5*	31.5	22.7	9.8	33.2	8.7*	16.0
	CL	12.4	5.0	11.0	8.5*	17.9	11.4	7.5*	14.0	11.0*
	CLT	12.3	4.6	16.7	11.2	17.3	11.5	10.1	14.3	12.3
	CLTP	10.8*	3.8*	18.5	11.8	13.7*	9.5*	10.1	13.7	11.5

Asterisks indicate the human condition that was most similar to chimpanzee gait.

elevated their pelvis on the swing side (Fig. 3C,D). The out-of-phase pattern of motion between the normal human condition and chimpanzee is reflected in the negative cross-correlation value (r=−0.80; Table 3). The pelvis list ROM was smaller in the CL and CLT posture conditions than in the normal condition (Table 2), and this relatively straight-line pelvis list trajectory resulted in r values that were close to zero for these conditions (CL: r=−0.11; CLT: r=0.05). For the CLTP condition, the human pelvis list pattern was in phase with the chimpanzee data (r=0.54) and had the most chimpanzee-like magnitude (RMSD=3.8 deg; Table 3).

Humans tilted their pelvis anteriorly for the normal posture condition, between −2 and −7 deg (Fig. 3E,F, Table 2). Chimpanzees also walked with a relatively vertical orientation of the pelvis, which resulted in a close match of the RMSD between the normal human condition and that of the chimpanzees (normal: RMSD=3.5 deg; Table 3). The different human posture conditions had little effect on the patterns of motion (r=[0.53, 0.58]; Table 3). However, during the crouched-posture conditions, humans tilted their pelvis anteriorly to a greater extent (CL: peak=−14 deg; CLTP: peak=−22 deg; Table 2) than for the normal condition. This resulted in greater RMSD values for the crouched human posture conditions than for the normal condition (CLTP: RMSD=18.5 deg; Table 3). In summary, the pelvis rotation and pelvis list motions were most chimpanzee-like in the CLTP condition; however, the pelvis tilt kinematics were less chimpanzee-like in the crouched-posture conditions compared with the normal human walking.

Lower/hind limb kinematics

In the normal human posture condition, humans began in hip flexion, gradually extended the hip throughout the stance phase to hyperextension (i.e. <0 deg hip flexion), then gradually flexed the hip again during the swing phase. During the human crouched-posture conditions, the hip was more flexed throughout the stride compared with the normal human condition (Table 2, Fig. 4A,B). Hip flexion was more similar in pattern (CLTP: r=0.99) and magnitude (CL: RMSD=8.5 deg) to that of chimpanzees in the human crouched-posture conditions than during the normal human condition (Table 3). There were only small differences in hip flexion motion across the different human crouched-posture conditions.

In the frontal plane, humans began the gait cycle in an abducted hip position, with adduction during the early part of stance phase, then abduction during the late stance phase (Fig. 4C,D). In contrast, chimpanzees maintained their hip in an abducted position throughout the stance and swing phases with a magnitude that exceeded the peak human hip abduction angle. Across the human crouched-posture conditions, humans had greater hip abduction than in the normal human condition, although it did not reach the same magnitude of hip abduction as in the chimpanzees (peak abduction angle: chimpanzees −31±4 deg; human CLTP −15 ±6 deg). The CLTP condition produced the most similar hip abduction pattern (r=0.99) and magnitude (RMSD=13.7 deg) to that of the chimpanzees (Table 3).

Both humans and chimpanzees internally rotated their hip during the stance phase and externally rotated their hip during swing (Fig. 4E,F). However, as was seen for the pelvis rotation, the chimpanzees had greater ROM (42±3 deg) than for any of the human conditions (greatest ROM for CLTP 17±4 deg). There were only subtle differences in hip rotation across the human posture conditions, with the CLTP condition producing the most chimpanzee-like hip rotation patterns (r=0.95) and magnitude (RMSD=9.5 deg; Table 3).

In the normal human condition, humans had a knee angle close to full extension throughout most of the stance phase, in contrast to the chimpanzees, which had a flexed knee angle throughout the gait cycle. The knee angle pattern was more similar to that of chimpanzees in each of the human crouched-posture conditions (r=0.99; Table 3) than in the normal human condition (Fig. 4G,H). The magnitude of knee angle in the crouched-posture conditions (CL: RMSD=7.5 deg) was also more similar to the magnitude of the chimpanzee knee angle than in the normal human condition (RMSD=33.2 deg).

In the normal human condition, humans rapidly plantar flexed the ankle early in the stance phase, gradually dorsiflexed the ankle throughout midstance, followed by a rapid plantar flexion motion at the end of stance phase (Fig. 4I ,J). The ankle angle patterns were more chimpanzee-like in the human crouched-posture conditions than in the normal condition (normal: r=0.61; CLTP: r=0.76). However, the ankle was more dorsiflexed throughout stance phase in the crouched-posture conditions than in the normal condition, resulting in a greater RMSD for the crouched-posture conditions (normal: RMSD=8.7 deg; CLTP: RMSD=13.7 deg).

Trunk kinematics

Human subjects maintained a nearly upright trunk segment angle in normal gait (−5.6±4.0 deg; Fig. 5A), while in the CL condition, humans had a greater trunk flexion angle (−24.3±14.0 deg) than in the normal condition. When given specific instructions to tilt forward at the trunk in the CLT and CLTP conditions, the human subjects averaged a trunk flexion angle of −38.0±9.6 deg in the CLT condition and −37.2±10.6 deg for the CLTP condition. For each of the CL, CLT and CLTP conditions, the forward flexion of the trunk was achieved through a combination of pelvis tilt (Fig. 3E) and lumbar flexion (Fig. 5B).

Journal of Experimental Biology (2022) 225, jeb243272. doi:10.1242/jeb.243272

GRFs

The vertical GRF had a double-peaked pattern in the normal human condition (Fig. 6A,B). During the human crouched-posture conditions, the vertical GRF still had a double-peaked shape but had a reduced second peak, and less of a trough between the peaks, compared with the normal human condition. The average chimpanzee vertical GRF pattern had only one distinct peak, which occurred in the first half of stance phase. The pattern and magnitude of the vertical GRFs were less similar between the normal human condition (r=0.97; RMSD=0.21) and chimpanzees than were each of the crouched human postures and chimpanzees (r=0.99; RMSD=0.13–0.14) (Table 4).

The gait of both humans and chimpanzees had a negative, posteriorly directed GRF during the first half of stance phase, then a positive, anteriorly directed GRF for the second half of stance phase (Fig. 6C,D). The vertical force during the second half of stance was different between humans and chimpanzees, as the peak positive GRF for the human conditions was greater than that of the chimpanzees. When compared with the normal human condition, the human crouched-posture conditions produced only slightly more chimpanzee-like AP GRF patterns (normal: r=0.85; CLTP: r=0.91) and magnitudes (normal: RMSD=0.05; CLTP: RMSD=0.04).

The human crouched-posture conditions produced greater medial GRFs throughout midstance than in the normal human condition, but the peak magnitude did not approach the magnitude for the chimpanzees (Fig. 6E,F). When compared with each of the human conditions, chimpanzees produced greater medial GRFs throughout the middle of stance phase. The pattern of ML GRF was more chimpanzee-like in the human crouched-posture conditions than in the normal human condition (normal: r =0.83; CLTP: r=0.92); however, the RMSD magnitude did not vary across any of the human posture conditions (RMSD=0.02). Overall, in all three planes of GRF, the GRFs were more chimpanzee-like in the human crouched postures than in the normal human condition, but the human crouched postures did not produce a monophasic vertical GRF as in chimpanzees.

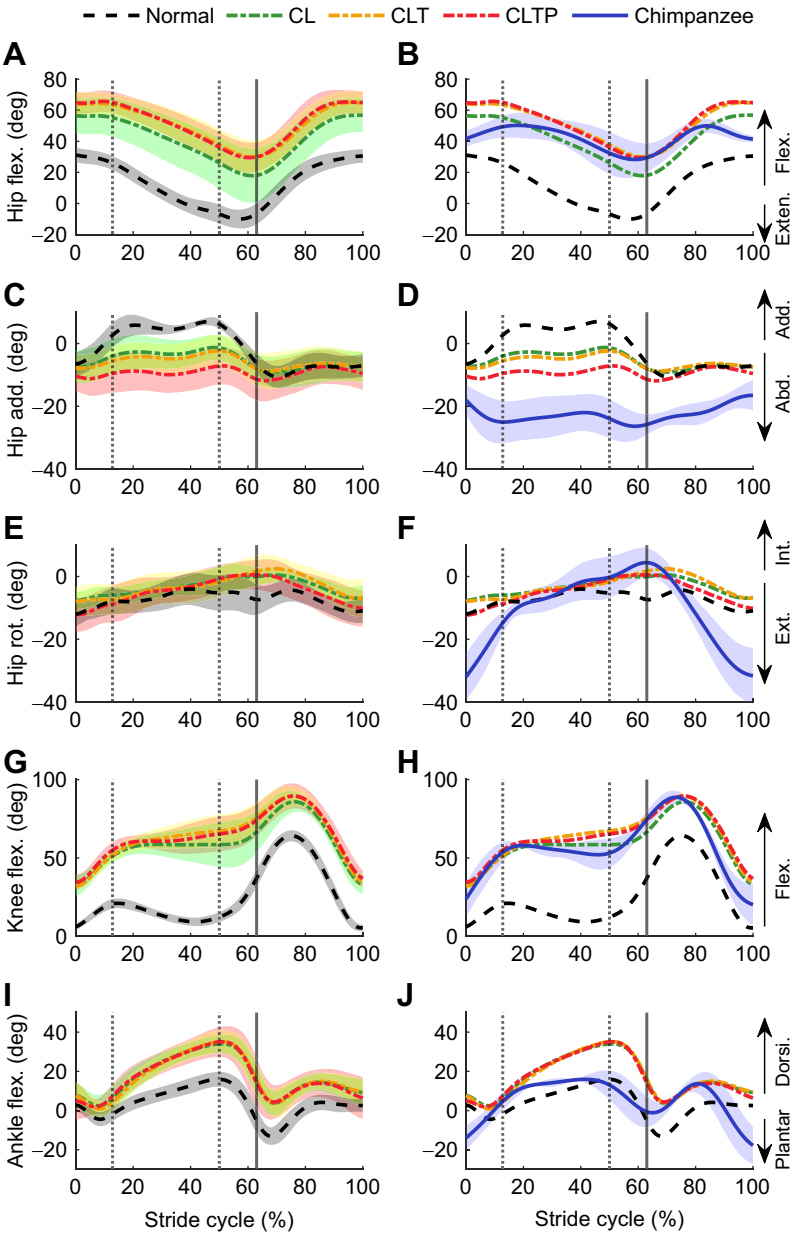

Fig. 4. Hind limb kinematics. Left: mean hip flexion (A), hip adduction (C), hip rotation (E), knee flexion (G) and ankle flexion (I) kinematics for each of the four human conditions (chimpanzee matched-speed; normal, CL, CLT, CLTP); shaded regions represent 1 s.d. of the mean. Right: mean hip flexion (B), hip adduction (D), hip rotation (F), knee flexion (H) and ankle flexion (J) kinematics for each of the four human conditions along with the mean and s.d. for the chimpanzee data. Exten., extension; Flex., flexion; Add., adduction; Abd., abduction; Int., internal; Ext., external; Dorsi., dorsiflexion; Plantar, plantarflexion.

Journal of Experimental Biology (2022) 225, jeb243272. doi:10.1242/jeb.243272

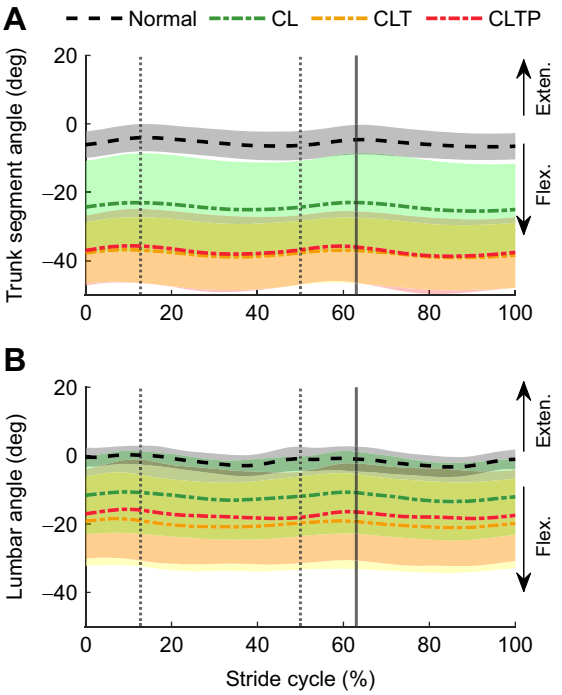

Fig. 5. Lumbar joint and trunk segment angles. The trunk segment angles (A) and lumbar joint angles (B) for each of the four human conditions (chimpanzee-matched speed; normal, CL, CLT, CLTP). Trunk angles were calculated as the sum of pelvis tilt and lumbar extension.

Average *r* and RMSD for kinematics and GRFs

Each of the human crouched-posture conditions produced more chimpanzee-like gait mechanics than the normal human condition according to each of the four metrics used to evaluate similarity (average *r* and RMSD for the kinematics and GRFs, respectively). Thus, the instructions provided to the subjects were generally effective at producing more chimpanzee-like gait mechanics than normal human gait. When evaluating how closely the three different crouched-posture conditions replicated chimpanzee gait, there were fewer generalizations that could be drawn. For the kinematic patterns, evaluated by the average *r*, the kinematic patterns in the CLTP condition were more chimpanzee-like than the other three conditions. The hip flexion, hip adduction and hip rotation had *r* values greater than 0.95 in the CLTP condition, which indicates a high similarity in pattern to the chimpanzee data for the hip angles. Compared with the CL condition, the CLT condition with the forward trunk flexion instruction did not further increase *r* values. For the other average metrics (kinematic RMSD, GRF *r* and RMSD), there was no single condition that most closely matched the chimpanzee data across all metrics. Additionally, for some variables such as pelvis rotation and ankle flexion, the crouched-posture conditions did not result in a close match to the chimpanzee data in *r* or RMSD. Overall, as can be observed by comparing the sizes of the standard deviation bands in Figs 3, 4 and 5, there was more variance in the human crouched-posture conditions, which could be due to the relatively unfamiliar nature of these tasks. While the crouched-posture instructions produced a more chimpanzee-like gait than normal human gait overall, the three crouched-posture conditions did not result in additive changes to gait mechanics that progressively better matched the bipedal chimpanzee mechanics, as hypothesized.

DISCUSSION

We compared the 3D gait mechanics of normal walking and crouched-posture walking in humans with bipedal walking in chimpanzees to understand the degree to which human crouched-posture walking is similar to that of bipedal chimpanzees walking. Our first hypothesis was that the normal human condition would be least like the chimpanzee gait mechanics compared with any of the crouched-posture conditions. Our data support this hypothesis as the normal human walking condition had the smallest average *r* and greatest average RMSD values for the kinematics and GRFs compared with each of the other human crouched postures. While each of the human crouched-posture conditions produced more chimpanzee-like gait mechanics than normal human walking, there was not strong support for the hypothesis that the human CLT condition would be more similar to chimpanzees than the human CL condition, as the gait mechanics between these conditions were similar. Our final hypothesis was that the joint kinematics and GRFs from the human CLTP condition would be most similar to the chimpanzee gait mechanics. The results for this hypothesis were more nuanced. The human CLTP condition did result in the most chimpanzee-like kinematic patterns (as measured by *r*). However, all three crouched-posture conditions had similar patterns (*r*) for the GRFs, and similar magnitude differences (RMSD) for both kinematics and GRFs. The greater average *r* value for the kinematic variables in the CLTP condition than the CL or CLT conditions was mostly driven by a more chimpanzee-like pelvis list pattern, corresponding with the instructions to modify the pelvis list motion.

Pelvis kinematics

Across all human posture conditions, one of the persistent kinematic differences between humans and chimpanzees was the pelvis transverse plane rotation ROM (Fig. 3B, Table 2). On average, chimpanzees had 41 deg of pelvis rotation ROM, while humans had a pelvis rotation ROM between 12 and 23 deg across the four conditions. Pelvis rotation can be linked with overall stride length, as greater pelvis rotation can lead to a greater stride length (Saunders et al., 1953; Whitcome et al., 2017). While chimpanzees have a greater range of pelvis rotation during their gait, humans did not increase pelvis rotation when walking with the CL or CLT postures. The pelvis rotation ROM was moderately greater in the CLTP posture relative to the other crouched limb postures (i.e. CLTP: 23 ±9 deg ROM; CLT: 15±6 deg ROM), but that was still half of the measured pelvis rotation ROM for bipedal chimpanzees. Therefore, our data suggest that greater pelvis rotation ROM in chimpanzees than in humans may not be a direct result of walking with shorter limbs or a crouched posture per se. Instead, the differences in pelvis rotation may reflect differences in the musculoskeletal design of the pelvis between humans and chimpanzees, such as ilia orientation (e.g. Lovejoy, 2005; Lycett and von Cramon-Taubadel, 2013; Stern and Susman, 1983). Determination of individual muscle contributions to pelvis rotation in bipedal chimpanzees and humans would provide additional insight into this issue.

While the human crouched postures did not elicit chimpanzee-like pelvis transverse plane rotation, the pelvis list pattern was more chimpanzee-like across all human crouched postures compared with normal human gait, even though the CL and CLT instructions only targeted sagittal plane variables. The pelvis list patterns for normal human gait and bipedal chimpanzee gait are out of phase (Fig. 3D), but the pelvis list pattern in the human crouched-posture conditions was in phase with the chimpanzee pelvis list pattern. This indicates that an important determinate of raising the pelvis on the limb swing side is walking on a flexed lower limb, possibly to aid with

Journal of Experimental Biology (2022) 225, jeb243272. doi:10.1242/jeb.243272

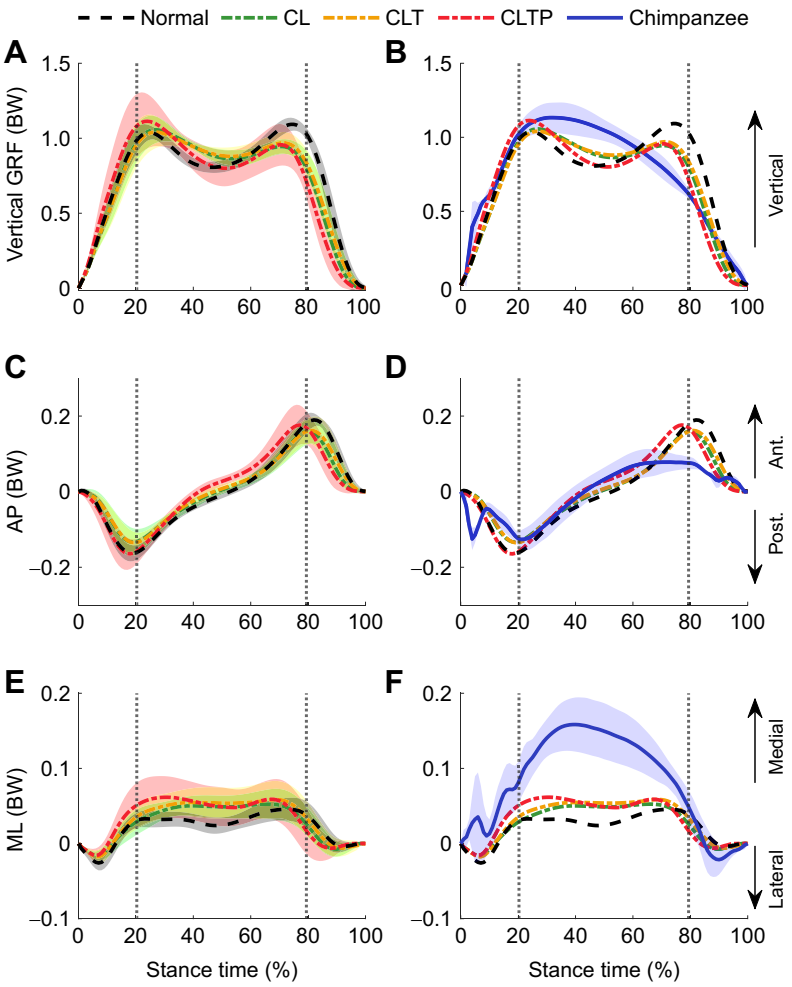

Fig. 6. Ground reaction forces (GRFs). Left: mean GRFs for the vertical (A), anterior–posterior (AP; C) and medial–lateral (ML; E) directions for each of the four human conditions (chimpanzee-matched speed; normal, CL, CLT, CLTP); the shaded regions represent 1 s.d. of the mean. Right: mean GRFs for the vertical (B), anterior–posterior (D) and medial–lateral (F) directions for each of the four human conditions along with the mean and s.d. for the chimpanzee data. BW, body weight.

foot–ground clearance (O'Neill et al., 2015, 2018). This also suggests that previous studies of human crouched-posture walking likely produced some degree of chimpanzee-like frontal plane pelvis motion, even if they did not measure it. However, the pelvis list motion was more chimpanzee-like in the CLTP condition than in the CL or CLT conditions, which suggests that the pelvis list pattern of bipedal chimpanzees may be due to other factors beyond that of simply walking with a crouched posture. Our current experimental design does not allow us to determine what causes the different degrees of pelvis tilt among the crouched postures. More human-based experiments could provide additional insight into the interaction, or lack thereof, between pelvis list and lower limb gait mechanics, perhaps by providing different instructions to humans to modify pelvis motion (e.g. Kikel et al., 2020), or by manipulating human anthropometrics (e.g. artificially increase foot length), which would affect foot–ground clearance during the swing phase of gait.

Table 4. Cross-correlation coefficients (*r*) and RMSD for ground reaction forces (GRFs) of humans walking (chimpanzee-matched speed) compared with chimpanzee gait

	Human condition vs chimpanzee	Vertical GRF	AP GRF	ML GRF	Average
r	Normal	0.97	0.85	0.83	0.88
	CL	0.99*	0.88	0.91	0.92
	CLT	0.99*	0.87	0.91	0.92
	CLTP	0.99*	0.91*	0.92*	0.94*
RMSD (BW)	Normal	0.21	0.05	0.02*	0.09
	CL	0.13*	0.04*	0.02*	0.06*
	CLT	0.13*	0.04*	0.02*	0.07
	CLTP	0.14	0.04*	0.02*	0.07

AP, anterior–posterior; ML, medial-lateral; BW, body weight. Asterisks indicate the human condition that was most similar to chimpanzee gait.

Humans walked with greater anterior pelvis tilt during all crouched-posture conditions compared with normal walking (Fig. 3E). In the normal walking condition, the pelvis tilt exhibited by humans overlapped the chimpanzee data, with both generally falling within ±5 deg of the upright, neutral position. In contrast, the differences in pelvis tilt kinematics between humans and chimpanzees were greater in the crouched postures. The greater forward pelvis tilt used by humans in the crouched-posture conditions, especially in the CL condition (tilted anteriorly 11–14 deg; Table 2), is a bit more similar to bipedal macaques (tilted anteriorly 8–13 deg) than to bipedal chimpanzees (Ogihara et al., 2010; O'Neill et al., 2018).

Lower/hind limb kinematics

The human sagittal plane hip and knee angles matched closely with the bipedal chimpanzee gait mechanics across each of the crouched-posture conditions (Fig. 4B,H). Most of the previous crouched-posture studies have focused on these two angles in particular, often referring to the gait pattern itself as 'bent-hip, bent-knee' (Carey and Crompton, 2005; Crompton et al., 1998; Foster et al., 2013;

Wang et al., 2003). Our dataset is the first to directly compare joint kinematics of human crouched-posture walking with that of bipedal chimpanzees; therefore, these data provide an important context for interpreting the results of previous studies, especially our CL condition, which replicates the experimental designs used in some prior research (Carey and Crompton, 2005; Foster et al., 2013). The remaining differences observed in our data for both kinematics and GRFs illustrate that instructing humans to adopt a 'bent-hip, bent-knee' walking posture results in an overall gait pattern that is still quite different from that of bipedal chimpanzee walking.

In normal human walking, the hip joint is adducted for most of the stance phase. In contrast, all three of the human crouched-posture conditions resulted in an abducted hip position throughout the gait cycle. Additionally, humans had greater hip abduction during stance in the CLTP condition than in the other crouched postures (Fig. 4C, Table 2), supporting previous results that swing side pelvis elevation (i.e. pelvis list) results in greater hip abduction (Kikel et al., 2020). However, the magnitude of the hip abduction angle across all crouched postures was still much less than that of chimpanzees (Fig. 4D). One potential explanation for the difference in the magnitude of the hip abduction angle is the presence of a frontal plane, valgus knee alignment in humans, which chimpanzees lack (Shefelbine et al., 2002; Tardieu and Trinkaus, 1994). A valgus knee enables humans to place their foot underneath the body center of mass throughout the stance phase, while maintaining an adducted hip position and with minimal upper body motion. The differences in knee alignment may allow the human subjects in this study to perform the crouched-posture conditions with less hip abduction than in the chimpanzees during bipedal gait. Likewise, *Australopithecus afarensis* had a valgus knee (Heiple and Lovejoy, 1971; Shefelbine et al., 2002), which suggests that regardless of the uncertainty in their posture (crouched versus upright) they likely walked with less hip abduction than chimpanzees.

The differences in hip transverse plane rotation ROM between humans and chimpanzees persisted throughout all human crouched-posture conditions. Humans averaged between 11 and 16 deg ROM across conditions, compared with 39 deg ROM for bipedal chimpanzees (Table 2). This persistent difference in hip rotation between humans and chimpanzees was similar to the persistent difference in pelvis transverse plane rotation for all human conditions compared with chimpanzees. However, one must be cautious in associating joint and segment motion when the femur is oriented ∼45 deg relative to vertical in crouched limb walking, rather than being nearly vertical in upright walking. Specifically, pelvis transverse plane rotation, as well as pelvis list, will be directly influenced by both hip joint adduction and hip joint rotation in ways that are hard to decipher without conducting a 3D kinematic analysis, as is reported here. For example, even with more chimpanzee-like pelvis list during human crouched-posture walking, these conditions do not result in chimpanzee-like hip joint adduction or hip joint rotation in humans. This is functionally importantly, as hip joint orientation is what will impact the leverage and function of the hip muscles to provide balance, support and propulsion during walking (i.e. Stern, 1972; Stern and Susman, 1981).

At the ankle, humans maintained a substantially more dorsiflexed ankle position throughout most of the stance phase in the crouched-posture conditions than for either normal human walking or bipedal walking in chimpanzees (Fig. 4I,J). As with the pelvis tilt kinematics, the ankle joint represents another case where the human crouched-posture conditions resulted in less chimpanzee-like kinematics than normal human walking. Because of the dorsiflexed ankle position at initial foot–ground contact in all conditions, humans contact the ground with their heel first (i.e. with a distinct heel strike) even when walking in the crouched postures. This early stance phase behavior is distinct from that of bipedal chimpanzees, which adopt a plantar flexed ankle angle at foot strike at initial foot–ground contact (O'Neill et al., 2015). This implies that the previously observed difference in foot strike patterns between humans and bipedal chimpanzees (O'Neill et al., 2015; O'Neill et al., 2018; O'Neill et al., 2022 preprint) is not simply a result of differences in lower limb flexion between species.

Trunk kinematics

There were only minor differences in the pelvis and lower limb kinematics between the CL and CLT conditions, demonstrating that an anteriorly flexed trunk does not substantially alter gait mechanics when humans walk with a crouched posture. While the trunk segment angles matched closely with our target trunk angle of −30 deg (Fig. 5A), humans achieved this segment angle through a combination of lumbar flexion (Fig. 5B) and pelvis tilt (Fig. 3E). The human subjects did this rather than maintaining a vertically oriented pelvis and flexing their vertebral column alone, as in bipedal chimpanzees (O'Neill et al., 2015). The incorporation of greater anterior pelvis tilt resulted in greater hip flexion angles throughout the gait cycle in the CLT condition than in the CL condition. The lack of broad differences in kinematics between CL and CLT conditions agrees with previous research on the effect of a moderately flexed trunk angle on crouched gait mechanics (Grasso et al., 2000).

Other researchers have examined the isolated effect of trunk orientation on gait mechanics and found that an anteriorly flexed trunk angle of 30 deg, without any instructions to modify lower limb posture, resulted in greater knee flexion and ankle dorsiflexion angles throughout stance than normal walking (Aminiaghdam et al., 2017; Kluger et al., 2014; Saha et al., 2008). While the 30 deg trunk flexion gait resulted in a crouched-limb posture in the study of Aminiaghdam et al. (2017), more extreme changes in gait mechanics occurred at trunk flexion angles of 90 deg. Given the recent focus on the length of the lumbar spine in hominin evolution (Lovejoy and McCollum, 2010; O'Neill et al., 2018; Williams and Russo, 2015), the results of our study provide some evidence that the orientation of the trunk is just one factor, among many, that impacts 3D gait kinematics, rather than the *sine qua non*. However, compared with humans, chimpanzees have a greater relative trunk size and a higher center of mass location of their trunk (Crompton et al., 1996), and more work is needed to evaluate how the combined effects of mass distribution and anterior trunk flexion affect gait mechanics.

GRFs

Consistent with the kinematic results, the GRFs were more chimpanzee-like in the human crouched-posture conditions than in the normal human gait condition. The GRFs in the crouched-posture conditions exhibit a greater first peak of the vertical GRF than second peak and a less prominent trough during mid-stance, as in previous studies (Aminiaghdam et al., 2017; Grasso et al., 2000; Saha et al., 2008). Yet, these GRF patterns were still quite distinct from those of bipedal chimpanzees, which exhibit a monophasic vertical GRF peak along with a smaller propulsive AP GRF at matched speeds (see also O'Neill et al., 2022 preprint). This indicates that crouched-posture walking is insufficient to account for differences in vertical and AP GRFs or patterns between species,

in contrast to some earlier inferences (Li et al., 1996). The differences in vertical GRFs between the crouched-posture human gaits and that of the chimpanzees suggest that the human crouch-posture COM motion is also distinct from both normal walking and bipedal chimpanzee walking, but additional analyses are required.

In human gait, the second vertical GRF peak and propulsive AP GRF peak are dominated by ankle plantar flexors (e.g. Liu et al., 2008; Winter, 1983). In bipedal chimpanzee walking, there is a much smaller peak ankle power in the second double support period of the stance phase than in human walking (O'Neill et al., 2022 preprint). The fact that humans retain a distinct second vertical GRF peak in crouched walking may reflect fundamental differences in relevant musculoskeletal traits of the human ankle (e.g. enlarged soleus; O'Neill et al., 2013) and foot (e.g. greater midfoot mobility; Holowka et al., 2017) as compared with bipedal chimpanzees (O'Neill et al., 2022 preprint). Moreover, the vertical and AP push-off forces in human crouched-posture walking fall between those of normal human walking and bipedal chimpanzee walking (Fig. 6), which, combined with a distinct heel strike in human crouched-posture walking due to a dorsiflexed ankle angle (Fig. 4), suggest caution when inferring the habitual walking posture (upright or crouched) of extinct hominins from footprints, such as those preserved at Laetoli (e.g. Crompton et al., 2012; Hatala et al., 2016; Raichlen et al., 2010). Overall, these data show that human crouched-posture gait remains distinct from chimpanzee gait in several important domains (pelvis motion, ankle angles and GRFs) in ways that are likely critical to their utility in studies of the evolution of hominin bipedalism.

Limitations

One potential limitation of this study was the human subjects practiced each of the crouched-posture conditions for only several minutes, rather than using the gait patterns for extended periods. A relatively short practice time was used in part because humans can readily walk with crouched postures, and also to avoid the possibility of localized muscle fatigue in the limb extensor muscles that might affect how the subjects walked. As the crouched-posture conditions were not common tasks for the human subjects, it is possible that a longer practice session or adaptation period would elicit different gait mechanics from those observed in this study (Sánchez et al., 2021; Selgrade et al., 2017). However, we expect that any further changes in gait mechanics following a longer adaptation period would be minor, as research has suggested that broad learning of new gait patterns occurs rapidly, with only minor adjustments occurring after the first few minutes of the new gait (Mawase et al., 2013; McDougle et al., 2015). Additionally, this study built upon previous work by including instructions to modify human gait towards that of a chimpanzee in both the sagittal and frontal planes. It is possible that different types of feedback or instruction could be provided to the subjects to guide them towards an even more chimpanzee-like gait than what was observed in our data, such as additional instructions to imitate ankle kinematics or vertical GRFs. Future studies could implement multiple practice sessions or real-time visual feedback to further modify specific features of the kinematics or GRFs in human crouched-posture gait, which could also allow for a closer match between human crouched-posture and chimpanzee gait.

Another potential limitation of this study is that human subjects did not walk at the same dimensionless speed as the chimpanzees based on the differences in lower/hind limb length. Given standing hip height differences (humans: 0.88±0.04 m; chimpanzees: 0.39 ±0.02 m), a dimensionless speed condition would have required the human subjects to walk at approximately 1.65 m s^{-1}. During pilot testing, we found that human subjects had difficulty performing the crouched-posture conditions while walking at this faster speed. However, there were only minor differences in gait mechanics between the chimpanzee-matched (1.1 m s^{-1}) and preferred (1.3 m s^{-1}) speed conditions in this study (see Figs S1–S3 and Tables S1–S3), and human kinematics have been shown to be broadly similar for the chimpanzee dimensional-matched and dimensionless-matched speeds (O'Neill et al., 2015). Thus, we expect the general conclusions in this study would hold for a wide range of walking speeds.

Conclusion

Human crouched-posture conditions produced a more chimpanzee-like gait than did normal human gait in pelvis list, hip and knee flexion–extension. However, substantial interspecific differences were evident in pelvis transverse plane rotation, hip abduction–adduction and mediolateral rotation, ankle plantar flexion–dorsiflexion and 3D GRFs. These results suggest that human crouched-posture walking captures a rather limited subset of the characteristics of 3D kinematics and GRFs, even with more elaborate instructions than is typical for human studies of this type. As such, human crouched walking is an inadequate proxy for chimpanzee or facultative bipedalism, despite what has previously been implied (e.g. Carey and Crompton, 2005; Li et al., 1996; Wang et al., 2003; Yamazaki et al., 1979). Our study suggests that the typical instructions of using a 'bent-hip, bent-knee' gait pattern cannot overcome some of the constraints that are imposed by human anatomical structure. Understanding why differences persist, even when attempting to recreate chimpanzee-like gait mechanics, can lead to novel insights linking musculoskeletal structure with gait mechanics. In addition to musculoskeletal morphology and posture, other factors also likely play important roles in determining gait mechanics in humans and non-human primates, such as the motor control of motion, metabolic energy expenditure or dynamic stability and balance. Human crouched-posture experimental studies may be most fruitful when used to test general principles of human musculoskeletal function, such as motor control (e.g. Grasso et al., 2000) or determinates of the metabolic costs of walking (e.g. Foster et al., 2013). Altogether, this study provides a comprehensive dataset to illustrate the gait mechanics used by humans and chimpanzees during several instantiations of crouched-posture bipedal gait, and the remaining differences between these species demonstrate how the distinct morphology of each species can impact bipedal gait.

Acknowledgements

The authors thank R. Wedge for assistance with the human data collection. Thanks to K. Fuehrer for animal care and training.

Competing interests

The authors declare no competing or financial interests.

Author contributions

Conceptualization: R.T.J., M.C.O., B.R.U.; Methodology: R.T.J., M.C.O., B.R.U.; Validation: R.T.J.; Formal analysis: R.T.J.; Investigation: R.T.J.; Data curation: R.T.J.; Writing - original draft: R.T.J.; Writing - review & editing: R.T.J., M.C.O., B.R.U.; Visualization: R.T.J.; Supervision: M.C.O., B.R.U.; Project administration: R.T.J., B.R.U.; Funding acquisition: M.C.O., B.R.U.

Funding

This study was supported by the National Science Foundation (NSF) awards BCS 0935327 and BCS 0935321. Additional support was provided by a University of Massachusetts Amherst dissertation research grant.

Data availability

Average human and chimpanzee kinematic and ground reaction force data are available from SimTK: https://simtk.org/projects/chimphindlimb

References

Aminiaghdam, S., Rode, C., Müller, R. and Blickhan, R. (2017). Increasing trunk flexion transforms human leg function into that of birds despite different leg morphology. *J. Exp. Biol.* **220**, 478-486. doi:10.1242/jeb.148312

Baker, R. (2001). Pelvic angles: a mathematically rigorous definition which is consistent with a conventional clinical understanding of the terms. *Gait Posture* **13**, 1-6. doi:10.1016/S0966-6362(00)00083-7

Blumenbach. (1775). *De Generis Humani Varietate Nativa*. Vandenhoek et Ruprecht.

Carey, T. S. and Crompton, R. H. (2005). The metabolic costs of "bent-hip, bent-knee" walking in humans. *J. Hum. Evol.* **48**, 25-44. doi:10.1016/j.jhevol.2004.10.001

Crompton, R. H., Li, Y., Alexander, R. M. N., Wang, W. and Gunther, M. M. (1996). Segment inertial properties of primates: new techniques for laboratory and field studies of locomotion. *Am. J. Phys. Anthropol.* **99**, 547-570. doi:10.1002/(SICI)1096-8644(199604)99:4<547::AID-AJPA3>3.0.CO;2-R

Crompton, R. H., Weijie, L. Y. W., Günther, M. and Savage, R. (1998). The mechanical effectiveness of erect and "bent-hip, bent-knee" bipedal walking in Australopithecus afarensis. *J. Hum. Evol.* **35**, 55-74. doi:10.1006/jhev.1998.0222

Crompton, R. H., Pataky, T. C., Savage, R., D'Août, K., Bennett, M. R., Day, M. H., Bates, K., Morse, S. and Sellers, W. I. (2012). Human-like external function of the foot, and fully upright gait, confirmed in the 3.66 million year old Laetoli hominin footprints by topographic statistics, experimental footprint-formation and computer simulation. *J. R. Soc. Interface* **9**, 707-719. doi:10.1098/rsif.2011.0258

Delp, S. L., Anderson, F. C., Arnold, A. S., Loan, P., Habib, A., John, C. T., Guendelman, E. and Thelen, D. G. (2007). OpenSim: open-source software to create and analyze dynamic simulations of movement. *IEEE Trans. Biomed. Eng.* **54**, 1940-1950. doi:10.1109/TBME.2007.901024

DeSilva, J. M., Gill, C. M., Prang, T. C., Bredella, M. A. and Alemseged, Z. (2018). A nearly complete foot from Dikika, Ethiopia and its implications for the ontogeny and function of *Australopithecus afarensis*. *Sci. Adv.* **4**, eaar7723. doi:10.1126/sciadv.aar7723

Donelan, J. M., Kram, R. and Kuo, A. D. (2001). Mechanical and metabolic determinants of the preferred step width in human walking. *Proc. R. Soc. B* **268**, 1985-1992. doi:10.1098/rspb.2001.1761

Doran, D. M. (1992). Comparison of instantaneous and locomotor bout sampling methods: a case study of adult male chimpanzee locomotor behavior and substrate use. *Am. J. Phys. Anthropol.* **89**, 85-99. doi:10.1002/ajpa.1330890108

Elftman, H. (1944). The bipedal walking of the chimpanzee. *J. Mammal.* **25**, 67-71. doi:10.2307/1374722

Foster, A. D., Raichlen, D. A. and Pontzer, H. (2013). Muscle force production during bent-knee, bent-hip walking in humans. *J. Hum. Evol.* **65**, 294-302. doi:10.1016/j.jhevol.2013.06.012

Garber, C. E., Blissmer, B., Deschenes, M. R., Franklin, B. A., Lamonte, M. J., Lee, I. M., Nieman, D. C. and Swain, D. P. (2011). American College of Sports Medicine position stand. Quantity and quality of exercise for developing and maintaining cardiorespiratory, musculoskeletal, and neuromotor fitness in apparently healthy adults: guidance for prescribing exercise. *Med. Sci. Sports Exerc.* **43**, 1334-1359. doi:10.1249/MSS.0b013e318213fefb

Grasso, R., Zago, M. and Lacquaniti, F. (2000). Interactions between posture and locomotion: motor patterns in humans walking with bent posture versus erect posture. *J. Neurophysiol.* **83**, 288-300. doi:10.1152/jn.2000.83.1.288

Hatala, K. G., Demes, B. and Richmond, B. G. (2016). Laetoli footprints reveal bipedal gait biomechanics different from those of modern humans and chimpanzees. *Proc. Biol. Sci.* **283**. doi:10.1098/rspb.2016.0235

Heiple, K. G. and Lovejoy, C. O. (1971). The distal femoral anatomy of Australopithecus. *Am. J. Phys. Anthropol.* **35**, 75-84. doi:10.1002/ajpa.1330350109

Holowka, N. B., O'Neill, M. C., Thompson, N. E. and Demes, B. (2017). Chimpanzee ankle and foot joint kinematics: Arboreal versus terrestrial locomotion. *Am. J. Phys. Anthropol.* **164**, 131-147. doi:10.1002/ajpa.23262

Jenkins, F. A. (1972). Chimpanzee bipedalism: cineradiographic analysis and implications for the evolution of gait. *Science (New York, N.Y.)* **178**, 877-879. doi:10.1126/science.178.4063.877

Kikel, M., Gecelter, R. and Thompson, N. E. (2020). Is step width decoupled from pelvic motion in human evolution? *Sci. Rep.* **10**, 7806. doi:10.1038/s41598-020-64799-3

Kimura, T., Okada, M. and Ishida, H. (1977). Dynamics of primate bipedal walking as viewed from the force of foot. *Primates* **18**, 137-147. doi:10.1007/BF02382955

Kluger, D., Major, M. J., Fatone, S. and Gard, S. A. (2014). The effect of trunk flexion on lower-limb kinetics of able-bodied gait. *Hum. Mov. Sci.* **33**, 395-403. doi:10.1016/j.humov.2013.12.006

Lai, A. K. M., Arnold, A. S. and Wakeling, J. M. (2017). Why are antagonist muscles co-activated in my simulation? a musculoskeletal model for analysing human locomotor tasks. *Ann. Biomed. Eng.* **45**, 2762-2774. doi:10.1007/s10439-017-1920-7

Li, Y., Crompton, R. H., Alexander, R. M., Gunther, M. M. and Wang, W. J. (1996). Characteristics of ground reaction forces in normal and chimpanzee-like bipedal walking by humans. *Folia Primatol.* **66**, 137-159. doi:10.1159/000157191

Liu, M. Q., Anderson, F. C., Schwartz, M. H. and Delp, S. L. (2008). Muscle contributions to support and progression over a range of walking speeds. *J. Biomech.* **41**, 3243-3252. doi:10.1016/j.jbiomech.2008.07.031

Lovejoy, C. O. (2005). The natural history of human gait and posture. Part 1. Spine and pelvis. *Gait Posture* **21**, 95-112. doi:10.1016/j.gaitpost.2004.01.001

Lovejoy, C. O. and McCollum, M. A. (2010). Spinopelvic pathways to bipedality: why no hominids ever relied on a bent-hip-bent-knee gait. *Philos. Trans. R. Soc. Lond. Ser. B Biol. Sci.* **365**, 3289-3299. doi:10.1098/rstb.2010.0112

Lovejoy, C. O., Suwa, G., Spurlock, L., Asfaw, B. and White, T. D. (2009). The pelvis and femur of Ardipithecus ramidus: the emergence of upright walking. *Science (New York, N.Y.)* **326**, 71e1-71e6. doi:10.1126/science.1175831

Lu, T.-W. and O'Connor, J. J. (1999). Bone position estimation from skin marker co-ordinates using global optimisation with joint constraints. *J. Biomech.* **32**, 129-134. doi:10.1016/S0021-9290(98)00158-4

Lycett, S. J. and von Cramon-Taubadel, N. (2013). Understanding the comparative catarrhine context of human pelvic form: A 3D geometric morphometric analysis. *J. Hum. Evol.* **64**, 300-310. doi:10.1016/j.jhevol.2013.01.011

Mawase, F., Haizler, T., Bar-Haim, S. and Karniel, A. (2013). Kinetic adaptation during locomotion on a split-belt treadmill. *J. Neurophysiol.* **109**, 2216-2227. doi:10.1152/jn.00938.2012

McDougle, S. D., Bond, K. M. and Taylor, J. A. (2015). Explicit and implicit processes constitute the fast and slow processes of sensorimotor learning. *J. Neurosci.* **35**, 9568. doi:10.1523/JNEUROSCI.5061-14.2015

Napier, J. (1967). The antiquity of human walking. *Sci. Am.* **216**, 56-66. doi:10.1038/scientificamerican0467-56

Ogihara, N., Makishima, H. and Nakatsukasa, M. (2010). Three-dimensional musculoskeletal kinematics during bipedal locomotion in the Japanese macaque, reconstructed based on an anatomical model-matching method. *J. Hum. Evol.* **58**, 252-261. doi:10.1016/j.jhevol.2009.11.009

O'Neill, M. C., Lee, L.-F., Larson, S. G., Demes, B., Stern, J. T., , Jr and Umberger, B. R. (2013). A three-dimensional musculoskeletal model of the chimpanzee (*Pan troglodytes*) pelvis and hind limb. *J. Exp. Biol.* **216**, 3709-3723. doi:10.1242/jeb.079665

O'Neill, M. C., Lee, L.-F., Demes, B., Thompson, N. E., Larson, S. G., Stern, J. T., , Jr and Umberger, B. R. (2015). Three-dimensional kinematics of the pelvis and hind limbs in chimpanzee (Pan troglodytes) and human bipedal walking. *J. Hum. Evol.* **86**, 32-42. doi:10.1016/j.jhevol.2015.05.012

O'Neill, M. C., Demes, B., Thompson, N. E. and Umberger, B. R. (2018). Three-dimensional kinematics and the origin of the hominin walking stride. *J. R. Soc. Interface* **15**. doi:10.1098/rsif.2018.0205

O'Neill, M. C., Demes, B., Thompson, N. E., Larson, S. G., Stern, J. T. and Umberger, B. R. (2022). Adaptations for bipedal walking: musculoskeletal structure and three-dimensional joint mechanics of humans and bipedal chimpanzees (Pan troglodytes). *bioRxiv*. doi:10.1101/2022.02.21.481231

Pontzer, H., Raichlen, D. A. and Rodman, P. S. (2014). Bipedal and quadrupedal locomotion in chimpanzees. *J. Hum. Evol.* **66**, 64-82. doi:10.1016/j.jhevol.2013.10.002

Raichlen, D. A., Gordon, A. D., Harcourt-Smith, W. E. H., Foster, A. D. and Haas, W. R. (2010). Laetoli footprints preserve earliest direct evidence of human-like bipedal biomechanics. *PLoS ONE* **5**, e9769. doi:10.1371/journal.pone.0009769

Rose, J. and Gamble, J. G. (2005). *Human Walking*, 3rd edn. LWW.

Saha, D., Gard, S. and Fatone, S. (2008). The effect of trunk flexion on able-bodied gait. *Gait Posture* **27**, 653-660. doi:10.1016/j.gaitpost.2007.08.009

Sánchez, N., Simha, S. N., Donelan, J. M. and Finley, J. M. (2021). Using asymmetry to your advantage: learning to acquire and accept external assistance during prolonged split-belt walking. *J. Neurophysiol.* **125**, 344-357. doi:10.1152/jn.00416.2020

Sarringhaus, L. A., MacLatchy, L. M. and Mitani, J. C. (2014). Locomotor and postural development of wild chimpanzees. *J. Hum. Evol.* **66**, 29-38. doi:10.1016/j.jhevol.2013.09.006

Saunders, J., Inman, V. T. and Eberhart, H. D. (1953). The major determinants in normal and pathological gait. *J. Bone Joint Surg. Am.* **35**, 543-558. doi:10.2106/00004623-195335030-00003

Selgrade, B. P., Thajchayapong, M., Lee, G. E., Toney, M. E. and Chang, Y.-H. (2017). Changes in mechanical work during neural adaptation to asymmetric locomotion. *J. Exp. Biol.* **220**, 2993-3000. doi:10.1242/jeb.149450

Seth, A., Hicks, J. L., Uchida, T. K., Habib, A., Dembia, C. L., Dunne, J. J., Ong, C. F., DeMers, M. S., Rajagopal, A., Millard, M. et al. (2018). OpenSim: Simulating musculoskeletal dynamics and neuromuscular control to study human and animal movement. *PLoS Comput. Biol.* **14**, e1006223. doi:10.1371/journal.pcbi.1006223

Shefelbine, S. J., Tardieu, C., Carter, D. R. (2002). Development of the femoral bicondylar angle in hominid bipedalism. *Bone* **30**, 765-770. doi:10.1016/S8756-3282(02)00700-7

Stern, J. T. (1972). Anatomical and functional specializations of the human gluteus maximus. *Am. J. Phys. Anthropol.* **36**, 315-339. doi:10.1002/ajpa.1330360303

Stern, J. T. and Susman, R. L. (1981). Electromyography of the gluteal muscles in Hylobates, Pongo, and pan: Implications for the evolution of hominid bipedality. *Am. J. Phys. Anthropol.* **55**, 153-166. doi:10.1002/ajpa.1330550203

Stern, J. T., , Jr and Susman, R. L. (1983). The locomotor anatomy of Australopithecus afarensis. *Am. J. Phys. Anthropol.* **60**, 279-317. doi:10.1002/ajpa.1330600302

Tardieu, C. and Trinkaus, E. (1994). Early ontogeny of the human femoral bicondylar angle. *Am. J. Phys. Anthropol.* **95**, 183-195. doi:10.1002/ajpa.1330950206

Thomas, S., Reading, J. and Shephard, R. J. (1992). Revision of the Physical Activity Readiness Questionnaire (PAR-Q). *Can. J. Sport Sci.* **17**, 338-345.

Thompson, N. E. (2016). The evolution of upper body stability in hominins. *PhD thesis*, Stony Brook University.

Wang, W. J., Crompton, R. H., Li, Y. and Gunther, M. M. (2003). Energy transformation during erect and “bent-hip, bent-knee” walking by humans with implications for the evolution of bipedalism. *J. Hum. Evol.* **44**, 563-579. doi:10.1016/S0047-2484(03)00045-9

Warburton, D. E. R., Gledhill, N., Jamnik, V. K., Bredin, S. S. D., McKenzie, D. C., Stone, J., Charlesworth, S. and Shephard, R. J. (2011). Evidence-based risk assessment and recommendations for physical activity clearance: Consensus Document 2011. *Appl. Physiol. Nutr. Metab.* **36** Suppl. 1, S266-S298. doi:10.1139/h11-062

Waterson, R. H., Lander, E. S., Wilson, R. K., and **The Chimpanzee Sequencing and Analysis Consortium**. (2005). Initial sequence of the chimpanzee genome and comparison with the human genome. *Nature* **437**, 69-87. doi:10.1038/nature04072

Whitcome, K. K., Miller, E. E. and Burns, J. L. (2017). Pelvic rotation effect on human stride length: releasing the constraint of obstetric selection. *Anat. Rec.* **300**, 752-763. doi:10.1002/ar.23551

Williams, S. A. and Russo, G. A. (2015). Evolution of the hominoid vertebral column: the long and the short of it. *Evol. Anthropol.* **24**, 15-32. doi:10.1002/evan.21437

Winter, D. A. (1983). Energy generation and absorption at the ankle and knee during fast, natural, and slow cadences. *Clin. Orthop. Relat. Res.* **175**, 147-154. doi:10.1097/00003086-198305000-00021

Yamaguchi, G. T. and Zajac, F. E. (1989). A planar model of the knee joint to characterize the knee extensor mechanism. *J. Biomech.* **22**, 1-10. doi:10.1016/0021-9290(89)90179-6

Yamazaki, N., Ishida, H., Kimura, T. and Okada, M. (1979). Biomechanical analysis of primate bipedal walking by computer simulation. *J. Hum. Evol.* **8**, 337-349. doi:10.1016/0047-2484(79)90057-5

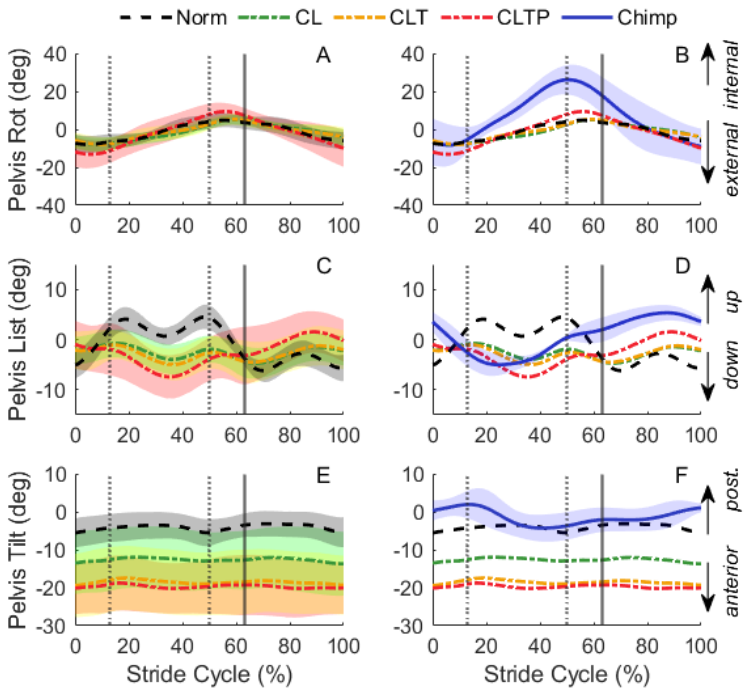

Fig. S1. Pelvis kinematics. The left column contains the pelvis rotation (A) list (C) and tilt (E) kinematics for each of the four human conditions at the preferred speed (Norm, CL, CLT, CLTP), with the shaded regions giving +/- 1 standard deviation. The right column shows the means for the pelvis rotation (B), list (D), and tilt (F) for each of the four human conditions along with the mean and standard deviation for the chimpanzee data (Chimp). The vertical lines depict left toe-off, left foot strike, and right toe-off respectively. Table S1 gives exact gait events across conditions.

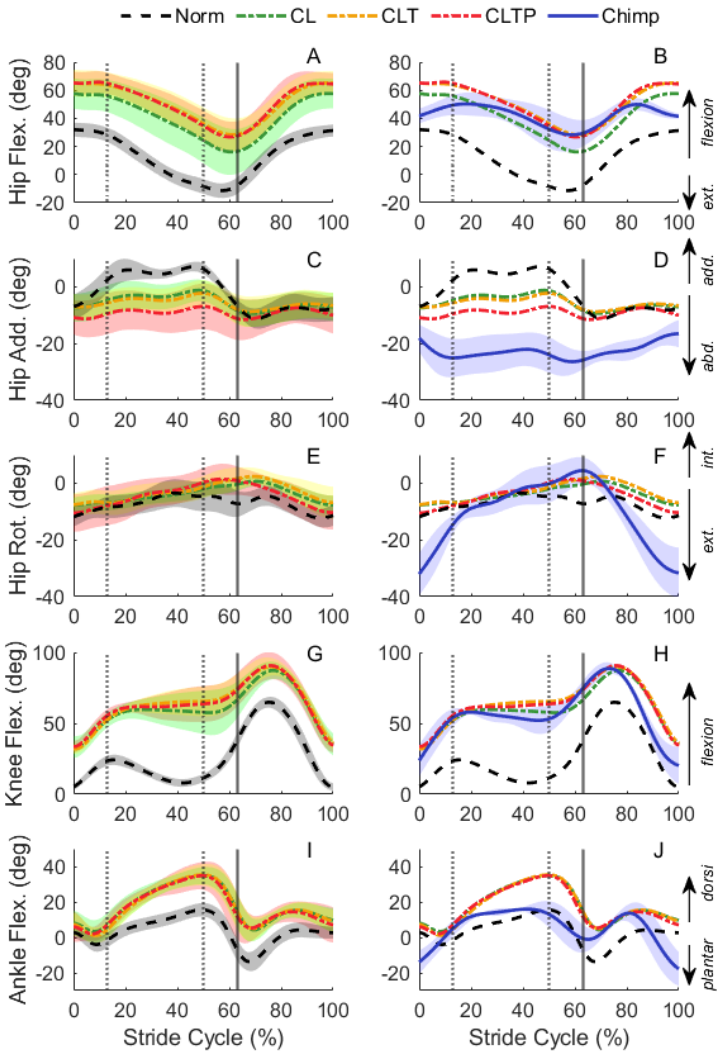

Fig. S2. Hind limb kinematics. The left column shows the hip flexion (A) hip adduction (C), hip rotation (E), knee flexion (G) and ankle flexion (I) kinematics for each of the four human conditions at the preferred speed (Norm, CL, CLT, CLTP), with the shaded regions giving +/- 1 standard deviation. The right column shows the means for the hip flexion (B) hip adduction (D), hip rotation (F), knee flexion (H) and ankle flexion (J) kinematics for each of the four human conditions along with the mean and standard deviation for the chimpanzee data (Chimp).

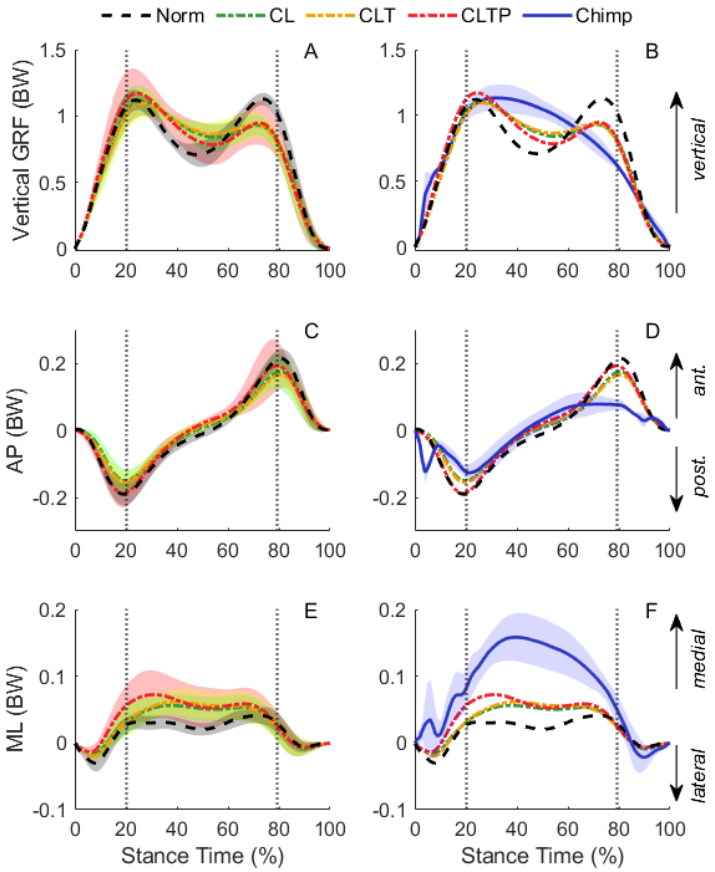

Fig. S3. Ground reaction forces (GRFs). The left column shows the ground reaction forces for the vertical (A) anterior-posterior (C), and medial-lateral (E) directions for each of the four human conditions at the preferred speed (Norm, CL, CLT, CLTP), with the shaded regions giving +/- 1 standard deviation. The right column shows the means for the ground reaction forces for the vertical (B) anterior-posterior (D), and medial-lateral (F) directions for each of the four human conditions along with the mean and standard deviation for the chimpanzee data (Chimp).

Table S1. Gait event timings (normalized to % stride time) for humans and chimpanzees.

	Left Toe Off	Left Foot Strike	Right Toe Off
Chimpanzee*	12.8 ± 1.7	49.0 ± 1.7	61.5 ± 3.1
Normal Chimp-Match	13.5 ± 1.4	50.8 ± 0.4	64.7 ± 1.2
Normal Preferred	13.1 ± 1.1	50.6 ± 0.4	64.4 ± 1.2
CL Chimp-Match	15.6 ± 1.4	51.2 ± 1.1	67.0 ± 1.3
CL Preferred	14.8 ± 1.4	51.4 ± 0.7	67.0 ± 1.4
CLT Chimp-Match	15.6 ± 1.6	51.5 ± 0.9	67.2 ± 1.3
CLT Preferred	14.7 ± 1.1	51.4 ± 1.1	66.8 ± 1.5
CLTP Chimp Match	14.4 ± 2.0	51.4 ± 1.2	66.3 ± 1.9
CLTP Preferred	13.5 ± 1.4	51.1 ± 1.0	65.3 ± 2.0

* Strides for chimpanzees begin at left heel strike, so data above are for right toe off, right foot strike, and left toe off, respectively.

Table S2. Zero-lag cross-correlation coefficients (*r*) and RMSD (units in degrees) for kinematics for humans walking with their preferred speed (1.31 ± 0.14 m/s) compared with chimpanzee gait (C); asterisks indicate human condition that was most similar to chimpanzee gait.

		Pelvis Rot.	Pelvis List	Pelvis Tilt	Hip F.	Hip Ad.	Hip R.	Knee	Ankle	Average
r	Normal v. C	0.59	-0.79	0.54	0.72	0.20	0.85	0.92	0.59	0.45
	CL v. C	0.39	-0.17	0.57	0.98	0.90	0.88	*0.99	0.73	0.66
	CLT v. C	0.50	-0.04	0.58	*0.99	0.95	0.84	*0.99	0.73	0.69
	CLTP v. C	*0.67	*0.48	*0.58	*0.99	*0.99	*0.97	*0.99	*0.77	*0.80
RMSD	Normal v. C	11.5	6.9	*3.5	31.7	22.6	*9.4	33.6	*8.9	15.9
	CL v. C	12.5	4.9	11.4	*9.4	17.8	11.2	*8.9	14.6	11.3
	CLT v. C	12.1	4.9	17.2	11.2	17.4	11.7	10.7	14.4	12.5
	CLTP v. C	*10.2	*3.8	18.4	11.6	*13.9	9.7	9.5	13.5	*11.3

Table S3. Cross-correlation coefficients (*r*) and RMSD (units in BW) for GRFs for humans walking with their preferred speed (1.31 ± 0.14 m/s) compared with chimpanzee gait (C); asterisks indicate human condition that was most similar to chimpanzee gait.

		Vertical GRF	AP GRF	ML GRF	Average
r	Normal v. C	0.96	0.86	0.79	0.87
	CL v. C	*0.99	0.88	0.91	0.93
	CLT v. C	*0.99	0.89	0.90	0.93
	CLTP v. C	*0.99	*0.90	*0.93	*0.94
RMSD	Normal v. C	0.22	0.06	*0.02	0.10
	CL v. C	0.12	*0.04	*0.02	*0.06
	CLT v. C	*0.11	*0.04	*0.02	*0.06
	CLTP v. C	0.14	0.05	*0.02	0.07